ical behavior of a nonlinear dumbbell model in steady shear flow. The time correlation functions that we derive in section III agree with their more general results. In addition, Jilge et al. (Jilge, W.; Hess, W.; Klein, R. *J. Polym. Sci., Polym. Phys. Ed.* **1983**, *23*, 1079) have studied the dynamic structure factor of linear dumbbells in shear flow.
(9) Dotson, P. J. *J. Chem. Phys.* **1983**, *79*(11), 5730.
(10) Stasiak, W.; Cohen, C. *J. Chem. Phys.* **1983**, *79*(11), 5718. Fuller, G. G. *J. Polym. Sci., Polym. Phys. Ed.* **1983**, *21*, 151. King, D. H.; James, D. F. *J. Chem. Phys.* **1983**, *78*(7), 4743. Lodge, A. S.; Wu, Y. *Rheol. Acta* **1971**, *10*, 539. van Wiechen, P. H.; Booij, H. C. *J. Eng. Math.* **1971**, *5*(2), 89. The last three papers exhibit general stationary-state solutions to the SE for a linear chain in an arbitrary flow field.
(11) Rouse, P. E. *J. Chem. Phys.* **1953**, *21*, 1272.
(12) Öttinger, H. C. *J. Chem. Phys.* **1986**, *84*(7), 4086. Öttinger, H. C. Preprint, Aug 1985. Honerkamp, J.; Öttinger, H. C. Preprint, Oct 1985. Biller, P.; Öttinger, H. C.; Petruccione, F. Preprint, Jan 1986. Öttinger, H. C. Preprint, Mar 1986.
(13) Fixman, M. *J. Chem. Phys.* **1966**, *45*(3), 793.
(14) Edwards, S. F.; Freed, K. F. *J. Chem. Phys.* **1974**, *61*(3), 1189.
(15) Stockmayer, W. H. In *Molecular Fluids*; Balian, R., Weill, G., Eds.; Gordon and Breach: New York, 1976.
(16) The Bose representation of a quantum harmonic oscillator can be found in many introductory quantum texts. See, for example: Merzbacher, E. *Quantum Mechanics*, 2nd ed.; Wiley: New York, 1961. Schiff, L. I. *Quantum Mechanics*, 3rd ed.; McGraw-Hill: New York, 1955.
(17) Guyer, R. A. *Phys. Rev. A* **1982**, *26*(2), 1062.
(18) Byron, F. W., Jr.; Fuller, R. W. *Mathematics of Classical and Quantum Physics*; Addison-Wesley: Reading, MA, 1969; Vol. I.
(19) Bird, R. B.; Saab, H. H.; Dotson, P. J.; Fan, X. J. *J. Chem. Phys.* **1983**, *79*(11), 5729.
(20) Johnson, J. A. Y. Ph.D. Thesis, University of Massachusetts, Amherst, MA, Feb 1985.
(21) de Gennes, P.-G. *Physics (Long Island City, N.Y.)* **1967**, *3*(1), 37.
(22) Brout, R.; Carruthers, P. *Lectures on the Many-Electron Problem*; Interscience: New York, 1963.
(23) Halmos, P. R. *Finite Dimensional Vector Spaces*, 2nd ed.; Van Nostrand: New York, 1958.
(24) Gradshteyn, I. S.; Ryzhik, I. M. *Table of Integrals, Series and Products* (corrected and enlarged edition); Academic: New York, 1980. Referred to as GR followed by the formula number.

Dynamics of an Entangled Chain in an External Field†

Douglas Adolf

Sandia National Laboratories, Albuquerque, New Mexico 87185. *Received June 17, 1986*

ABSTRACT: A straightforward model for the dynamics of an entangled macromolecule in an external field is presented. The model balances the frictional drag forces, random thermal forces, and the external body forces acting on a chain confined to a tube by entanglements with its neighbors. The calculated center-of-mass velocity is found to be in agreement with experiment and current theories, and the center-of-mass diffusion coefficients parallel and transverse to the external field are predicted to increase with increasing field strength. The time required for a chain to renew its configuration is predicted to decrease with increasing field strength. The results of a computer simulation based on this model are in agreement with theory.

Introduction

The self-diffusion of linear entangled polymers seems to be well described by the reptation theory of de Gennes.[1,2] Of present interest is the effect of an external body force on this mechanism of diffusion.[3-8] The most important example of this process is gel electrophoresis where DNA molecules of differing molecular weights that are forced through a gel by an applied electric field can be separated with extreme sensitivity. Of course, other body forces should have similar effects on the dynamic properties, and experiments to test this can be envisioned: gel sedimentation where a centrifugal force separates chains of different molecular weights and the self-diffusion of a tracer chain in a chemical potential gradient formed by the interdiffusion of two miscible polymers.

Several theories have been proposed to determine the dynamics of an entangled polymer in an external field. Those of Lumpkin and co-workers[3,4] and Slater and Noolandi[5,6] are based on modifications of the version of reptation set forth by Doi and Edwards.[9] In this model, an entangled chain is viewed as being trapped in a tube that prohibits motion perpendicular to its contour and, therefore, the chain is forced to follow the tube's contour by the set of equations

$$\mathbf{r}_n(t+\Delta t) = \{[1+\xi(t)]/2\}\mathbf{r}_{n+1}(t) + \{[1-\xi(t)]/2\}\mathbf{r}_{n-1}(t) \qquad (2 \le n \le N-1)$$

$$\mathbf{r}_1(t+\Delta t) = \{[1+\xi(t)]/2\}\mathbf{r}_2(t) + \{[1-\xi(t)]/2\}[\mathbf{r}_1(t)+\mathbf{v}(t)] \quad (1)$$

$$\mathbf{r}_N(t+\Delta t) = \{[1+\xi(t)]/2\}[\mathbf{r}_N(t)+\mathbf{v}(t)] + \{[1-\xi(t)]/2\}\mathbf{r}_{N-1}(t)$$

where $\mathbf{r}_i(t)$ is the position of the ith monomer at time t, $\mathbf{v}(t)$ is a random vector of segment length a, which defines the orientation of a terminal segment as it leaves the tube, and $\xi(t)$ is randomly 1 or −1, depending on which end of the chain leads. Lumpkin et al. calculated the center-of-mass velocity[4] and found agreement with experimental observations that the velocity is inversely proportional to the molecular weight for low molecular weights and is independent of it at higher values.[10-12] They were not, however, concerned with deriving a complete theory for the dynamics of entangled chains in an external field, as is the goal of the present study. Slater and Noolandi[5] do propose such a theory, and the differences between their theory and ours will be discussed later in this paper.

Olvera de la Cruz et al.[8] approached this problem in a completely different manner. They simulated an entangled macromolecule in an electric field by a chain moving via modified Verdier-Stockmayer dynamics[13,14] in the presence of a fixed obstacle net and an external field. The chain relaxation time in their simulation actually increased with increasing field strength. At first this result seems

†This work performed at Sandia National Laboratories supported by the U.S. Department of Energy under Contract No. DE-AC04-76DP00789.

0024-9297/87/2220-0116$01.50/0

to be counterintuitive, but it may be true, as pointed out by the authors,[8] for intense fields where the chain gets trapped in metastable configurations. The present study will focus on weaker fields where the dynamics are less dependent on the barriers associated with individual segments and are governed more by the cooperative modes described by the Doi–Edwards version of reptation.

Theory

Following the approach of Doi and Edwards, we assume that an entangled chain in an external field is confined to a tube. Accordingly, each segment of the chain will feel three forces tangential to the chain contour at that point: a frictional drag force, a random thermal force, and the external body force. The equation of motion for the chain is given by

$$Nm\, d^2s/dt^2 = -N\zeta\, ds/dt + (F_r/3^{1/2})\sum_{i=1}^{N}\chi_i(t) + F_eR_x/a \tag{2}$$

where s is the position of a monomer along the chain contour, m is the mass per segment, ζ is the monomer friction factor, F_r is the root mean square random force per segment, F_e is the magnitude of the external force per segment, and R_x is the component of the end-to-end vector parallel to the external force. In addition, $\chi_i(t)$ is a random variable with the following properties: $\langle\chi_i\rangle = 0$, $\langle\chi_i^2\rangle = 1$, $\chi_i(t_1)$ and $\chi_i(t_2)$ are uncorrelated except when $|t_1 - t_2|$ is very small, and $F_r^2\int_{-\infty}^{\infty}\langle\chi_i(t)\chi_i(0)\rangle\, dt = 6\zeta kT$, where T is the absolute temperature.[15] The factor of $1/(3)^{1/2}$ in the random force term arises from the fact that only the component of the random force per segment tangent to the chain contour is involved.

This equation can be simplified if the inertial term is neglected, as in the Rouse model for dilute dynamics,[16] and the total random force on the chain is approximated by

$$(F_r/3^{1/2})\sum_{1}^{N}\chi_i = (F_r\xi/3^{1/2})(\sum_{1}^{N}\langle\chi_i^2\rangle)^{1/2} = F_r\xi(N/3)^{1/2} \tag{3}$$

where $\xi(t)$ is defined to be randomly 1 or -1 as in the Doi–Edwards theory. Equation 2 then reduces to

$$\dot{s} \approx s/\Delta t = F_r\xi/\zeta(3N)^{1/2} + UF_rR_x/\zeta L \tag{4}$$

where U is the ratio of F_e/F_r and $L = aN$ is the tube length. In this discrete time representation, F_r^2 is equal to $6\zeta kT/\Delta t$, where Δt is a constant time increment, and s/a represents the number of segments that escape the tube during Δt and is not restricted to unity as in the Doi–Edwards theory. The sign of s, from eq 4, determines which end of the chain leads and is equal to

$$\text{sign}\,[1 + (UR_x/\xi a)(3/N)^{1/2}] \tag{5}$$

In other words, due to the external field, the probabilities for forward and backward motion in the tube are no longer equal.

The external field also causes an orientation of the segments as they exit the tube instead of the random orientation in the Doi–Edwards formulation. When inertial effects are neglected, the displacement of a bead as it leaves its tube is given by

$$\Delta\mathbf{r} = [(F_e/\zeta)\hat{\delta}_x + (F_r\cos\theta/\zeta)\hat{\delta}_x + (F_r\sin\theta\sin\phi/\zeta)\hat{\delta}_y + (F_r\sin\theta\cos\phi/\zeta)\hat{\delta}_z](\Delta t') \tag{6}$$

where $\hat{\delta}_i$ is the unit vector in the ith direction. However, $((\Delta\mathbf{r}\cdot\Delta\mathbf{r})^2)^{1/2}$ should be the length of a segment, a, so a normalizing factor is introduced. This is equivalent to moving the bead according the eq 6 for a distance, a, and then stopping. Therefore, the normalized segment displacement (i.e., the segment orientation) is given by

$$\Delta\mathbf{r} = \frac{U\hat{\delta}_x + \cos\theta\,\hat{\delta}_x + \sin\theta\sin\phi\,\hat{\delta}_y + \sin\theta\cos\phi\,\hat{\delta}_z}{(U^2 + 2U\cos\theta + 1)^{1/2}}a \tag{7}$$

The steady-state center-of-mass velocity can now be calculated by following the procedure of Lumpkin and Zimm.[3] First, the change in position of the center of mass, $\mathbf{R}_G$, in a time Δt is given by

$$\mathbf{R}_G(t + \Delta t) - \mathbf{R}_G(t) = \dot{s}(\Delta t)\mathbf{R}(t)/L \tag{8}$$

Inserting $\dot{s}$ from eq 4, summing over M time steps, and averaging result in

$$\langle\mathbf{R}_G(M\Delta t) - \mathbf{R}_G(0)\rangle = \sum_{i=0}^{M-1}\langle(F_r\xi/\zeta(3N)^{1/2} + UF_r/\zeta L)\mathbf{R}_i/L\rangle(\Delta t) \tag{9}$$

where $\mathbf{R}_i$ is the end-to-end vector at time $i\Delta t$. Noticing that $\langle\xi\rangle = 0$ and dividing by $t = M\Delta t$, we can express the average steady-state center-of-mass velocity in the direction of the external field, V_x, as

$$V_x = UF_r\langle R_x^2\rangle/\zeta L^2 \tag{10}$$

In a later paper, Lumpkin et al.[4] derive an expression for $\langle R_x^2\rangle/L^2$ for a chain of constant segment length. For weak fields ($F_e < F_r$), this quantity is given by

$$\langle R_x^2\rangle/L^2 = 1/3N + (E'/3)^2 \tag{11}$$

where E' is the ratio of the external field and the thermal energies. This ratio determines the average length of a segment in the direction of the field, $\langle a_x\rangle$, as it exits the tube. For weak fields, $\langle a_x\rangle$ equals $E'a/3$ in the Lumpkin et al. approach. In the present approach, however, the orientation of segments exiting the tube is calculated somewhat differently. The average length of a segment in the field direction, $\langle a_x\rangle$, can be found by integrating the x component of eq 7 over all angles. This calculation results in $\langle a_x\rangle = 2Ua/3$ for weak fields, so $E' = 2U$ and

$$\langle R_x^2\rangle/L^2 = 1/3N + (2U/3)^2 \tag{12}$$

The center-of-mass diffusion coefficient can be obtained in a similar manner. Following eq 8, we can express the mean square displacement of the center of mass in a time $t = M\Delta t$ for a steady-state process as

$$\langle[\mathbf{R}_G(t) - \mathbf{R}_G(0)]^2\rangle = \langle\Delta\mathbf{R}_G^2(t)\rangle = \sum_{i=0}^{M-1}\sum_{j=0}^{M-1}\langle(\dot{s}_i\mathbf{R}_i/L)\cdot(\dot{s}_j\mathbf{R}_j/L)\rangle(\Delta t)^2 \tag{13}$$

Substitution of eq 4 for $\dot{s}_k$ and δ_{ij} for $\langle\xi_i\xi_j\rangle$ reduces eq 13 to

$$\langle\Delta R_G^2(t)\rangle = (F_r/\zeta L)^2M\langle R^2\rangle(\Delta t)^2/3N + (F_e/\zeta L^2)^2\sum_{i=0}^{M-1}\sum_{j=0}^{M-1}\langle R_{xi}R_{xj}\mathbf{R}_i\cdot\mathbf{R}_j\rangle(\Delta t)^2 \tag{14}$$

Switching from discrete to continuous time results in

$$\langle\Delta R_G^2(t)\rangle = (F_r/\zeta L)^2\langle R^2\rangle(\Delta t)t/3N + (F_e/\zeta L^2)^2\int_0^t dt'\int_0^t dt''\, G(t',t'') \tag{15}$$

where $G(t',t'') = \langle R_x(t')R_x(t'')\mathbf{R}(t')\cdot\mathbf{R}(t'')\rangle$. In order to proceed further, the functional form of G must be known. Assume that in the steady state

$$G_x(t',t'') = [(\langle R_x^4\rangle - \langle R_x^2\rangle^2)e^{-|t'-t''|/\tau_P} + \langle R_x^2\rangle^2]$$

and

$$G_y(t',t'') = \langle R_x^2\rangle e^{-|t'-t''|/\tau_P}\langle R_y^2\rangle e^{-|t'-t''|/\tau_T} \quad (16)$$

where $G = G_x + G_y + G_z = G_x + 2G_y$. As shown later, these functional forms are not exact; however, the simulation results in the next section imply that the mean square center-of-mass displacement is not extremely sensitive to the exact form of G.

With these assumed relations, the mean square displacements of the center of mass parallel and perpendicular to the external field are given by

$$\langle \Delta X_G^2(t)\rangle \approx 2D_x t + V_x^2 t^2 \qquad \text{for } t > \tau_P$$

and

$$\langle \Delta Y_G^2(t)\rangle \approx 2D_y t \qquad \text{for } t > \tau_T \quad (17)$$

V_x is given by eq 10, and the diffusion coefficients are given by

$$D_x = D_{rep}\langle R_x^2\rangle/\langle R_x^2\rangle_0 + (UF_r/\zeta L^2)^2(\langle R_x^4\rangle - \langle R_x^2\rangle^2)\tau_P \quad (18)$$

and

$$D_y = D_{rep}\langle R_y^2\rangle/\langle R_y^2\rangle_0 + (UF_r/\zeta L^2)^2[\langle R_x^2\rangle\tau_P\tau_T/(\tau_P + \tau_T)]\langle R_y^2\rangle = D_{rep}\langle R_y^2\rangle/\langle R_y^2\rangle_0 + C(UF_r/\zeta)^2 \quad (19)$$

where $\langle R_i^2\rangle_0$ is the ith component of the mean square end-to-end vector when there is no external field, $D_{rep} = D/3N$ is the center-of-mass diffusion coefficient for a reptating chain (no external field), and D is the tube diffusion coefficient introduced by Doi and Edwards, which in this formlism is given by

$$D = (F_r/\zeta)^2(\Delta t/6N) = kT/\zeta N \quad (20)$$

Two points should be made concerning these results. First, the tube diffusion coefficient is proportional to N^{-1}, as expected. Second, the mean square displacement of the center of mass parallel to the external field approaches the square of the mean center-of-mass displacement at long times, as expected.

At this point, it is interesting to compare the present approach to that of Slater and Noolandi.[5] They too recognize that the possibility for forward or backward motion in the tube and the orientation of the exiting segments are biased when an external field is applied. However, they assume that the length of chain leaving the tube in a time Δt is independent of the external field. The forward and backward movement probabilities are determined so that the center-of-mass velocity is equivalent to that of Lumpkin et al.[4] (eq 10). The resulting probabilities for forward or backward motion are different from those in eq 5, but the center-of-mass velocity is correct by design. Whether or not the two procedures yield completely equivalent dynamics is unclear.

The decay of the correlation of the components of the end-to-end vector cannot be calculated by using the techniques described above. However, the correlation function, $\langle R_y(t)R_y(0)\rangle$, should be related to, but not identical with, the fraction of segments at time t still in the tube defined at time $t = 0$ (the original tube). To calculate this quantity, $F(t)$, it is first necessary to find the more detailed probability $f(t)$ that a segment starting at the origin at $t = 0$ will be found at a position η a time t later, subject to adsorbing boundary conditions at x and $x - L$. These boundary conditions ensure that the segment has not left the tube during the time t. The solution to this problem

$$\partial f/\partial t = D\partial^2 f/\partial\eta^2 - (F_e R_x/\zeta L)\partial f/\partial\eta$$

subject to the boundary conditions

$$f(\eta,0) = \delta(\eta) \qquad f(x,t) = f(x - L, t) = 0 \quad (21)$$

is

$$f(\eta,t) = (2/L)\sum_1^\infty \sin[n\pi(x - F_e\langle|R_x|\rangle t/\zeta)/L^2] \times \sin[n\pi(x - \eta)/L]e^{-n^2\pi^2 Dt/L^2} \quad (22)$$

This convective diffusion equation is the Smoluchowski equation corresponding to the Langevin equation of motion in eq 2.[17] The quantity R_x in eq 21 is actually time dependent; however, if we are concerned with times less than the longest relaxation time, R_x changes little and can be approximated by $\langle|R_x|\rangle$, as assumed in eq 22.

To find $F(t)$, it is necessary to integrate η from $x - L$ to L and then x/L from 0 to 1. (This procedure parallels that of Graessley,[18] who calculated $F(t)$ for a reptating chain.) The result is

$$F(t) = (8/\pi^2)\sum_{n\ \text{odd}} n^{-2}\cos(n\pi F_e\langle|R_x|\rangle t/\zeta L^2)\exp(-n^2 t/\tau_{rep}) \quad (23)$$

where $\tau_{rep} = L^2/\pi^2 D$ is the longest relaxation time for a reptating chain. This function reduces to the correct expression for a reptating chain when $F_e = 0$.[18]

It seems reasonable that the relaxation time for a chain in a strong external field should be equal to the ratio of the tube length, L, and the average curvilinear velocity, $\langle\dot{s}\rangle$, which is given by

$$\langle\dot{s}\rangle = UF_r\langle|R_x|\rangle/\zeta L \quad (24)$$

The dependence of the relaxation time on the external field reflects that the chain relaxes more quickly in stronger external fields. If eq 23 is rewritten in dimensionless form, where $\tau = t/\tau_{rep}$, $K = \tau_{rep}/\tau_e$, and $\tau_e = L^2\zeta/\pi F_e\langle|R_x|\rangle = L/\pi\langle\dot{s}\rangle$, then

$$F(t) = (8/\pi^2)\sum_{n\ \text{odd}} n^{-2}\cos(nK\tau)\exp(-n^2\tau) \quad (25)$$

Since this function is nonexponential, the relaxation time, τ_1, is operationally defined as the time where $F(\tau) = e^{-1}$. In Figure 1, τ_1 is plotted against K logarithmically. The dotted line has a slope of −1, showing that the relaxation time is indeed proportional to τ_e for large U (i.e., strong fields) as predicted.

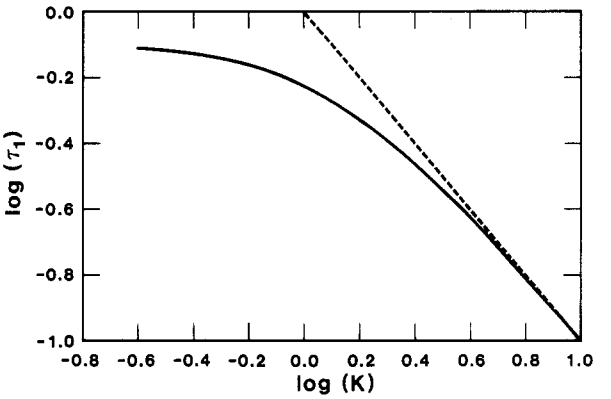

Figure 1. Relaxation time, τ_1, vs. $K \sim \tau_e^{-1}$ using eq 25. Dotted line has slope = −1, showing $\tau_1 \sim \tau_e$ for large U.

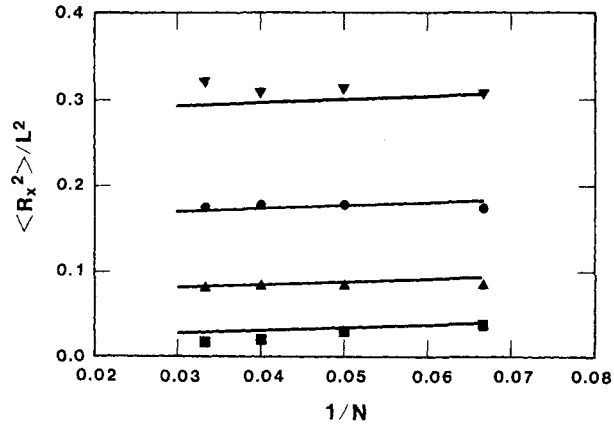

Figure 2. Ratio of the component of the mean square end-to-end vector in the direction of the field to the contour length squared vs. the reciprocal of the number of segments for differing field strengths. Points from simulation with $U = 0.2$ (■), $U = 0.4$ (▲), $U = 0.6$ (●), and $U = 0.8$ (▼). Lines are theory (eq 12) for the same parameter values.

Simulation

The dynamics of an entangled chain in an external field have been simulated on a VAX 11/750 using the approach discussed above. At every time step, a chain of N beads is moved such that bead i is moved to the position of bead $i + s/a$, where the magnitude of s is determined by eq 4. One difference between theory and simulation is that s/a can be continuous in the theory but is taken as the nearest integer in the simulation. This introduces an error, not associated with poor statistics, that becomes worse when s/a is small (i.e., weak external fields). Notice that s/a beads will be moved outside the tube defined at the beginning of that time step. The orientation of each bead exiting the tube is determined by eq 7. This approach requires three random numbers: one that is randomly 1 or −1, representing ξ in eq 4; one uniformly distributed between 0 and 2π, representing the arbitrary angle ϕ in eq 7; and one that is uniformly distributed between 0 and π, representing the arbitrary angle θ also in eq 7. Chains of 10, 20, 30, and 40 beads (each bead of length $a = 1$) in fields of strength $U = 0$, 0.2, 0.4, 0.6, and 0.8 with $F_r/\zeta = 11$ were simulated. Each simulation was run 1500 times the observed relaxationtime to ensure adequate statistics.

The chain statics can be examined in Figures 2–4. In Figure 2, $\langle R_x^2 \rangle / L^2$ is plotted against $1/N$, anticipating the functional relationship of eq 12. In fact, simulation (points) and theory (lines) from eq 12 are in good agreement. Equation 12 states that the parallel component of the mean square end-to-end vector elongates from its random walk value ($\sim N$) at $U = 0$ and becomes proportional to N^2 at large U. The transverse component of the mean square end-to-end vector is always proportional to the number of beads but decreases in magnitude slightly as U is increased. More specifically, the quantity $(\langle R_y^2 \rangle + \langle R_z^2 \rangle)/N = 0.762 \pm 0.012$ when $U = 0$ and decreases by about 20% to 0.598 ± 0.016 when $U = 0.8$.

The quantity $\langle |R_x| \rangle$ is plotted logarithmically against N and U in Figures 3 and 4. As expected, $\langle |R_x| \rangle$ is proportional to $N^{1/2}$ for small U (solid line slope = $^1/_2$ in Figure 3) and becomes proportional to N at high U (dotted line slope = 1 in Figure 3). Again, this is due to the external field elongating the chain in the direction of the field. The field dependence of $\langle |R_x| \rangle$ is shown in Figure 4. We see that for $U \geq 0.2$ $\langle |R_x| \rangle$ is proportional to U (slope of line = 1). At very high field strengths, $\langle |R_x| \rangle$ will be totally elongated and will become independent of U. This limit is not reached in the simulations.

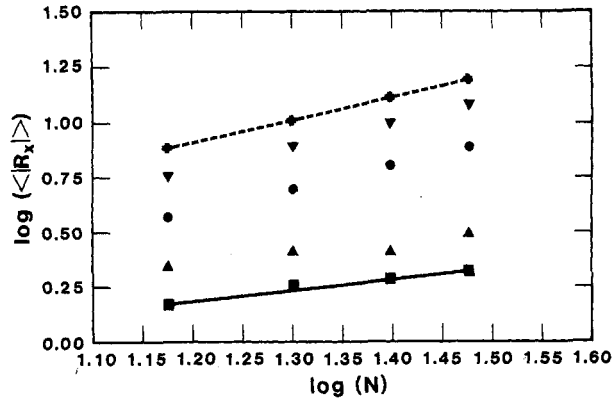

Figure 3. Simulation parallel component of the end-to-end distance vs. number of beads for $U = 0$ (■), $U = 0.2$ (▲), $U = 0.4$ (●), $U = 0.6$ (▼), and $U = 0.8$ (+). Solid line has slope of $^1/_2$ valid for $U = 0$, and dotted line has slope of 1 valid for large U.

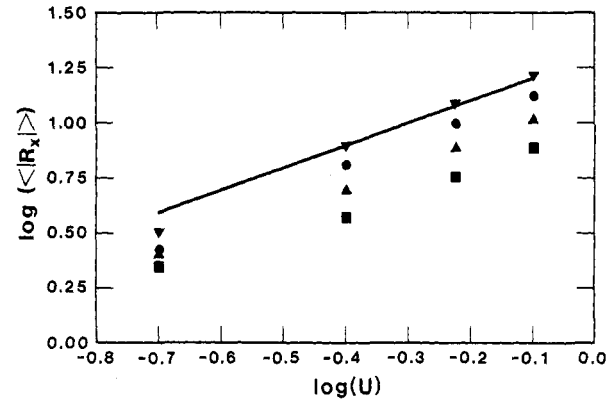

Figure 4. Simulation parallel component of the end-to-end distance vs. field strength for $N = 15$ (■), $N = 20$ (▲), $N = 25$ (●), and $N = 30$ (▼). Line has slope of 1 valid for large U.

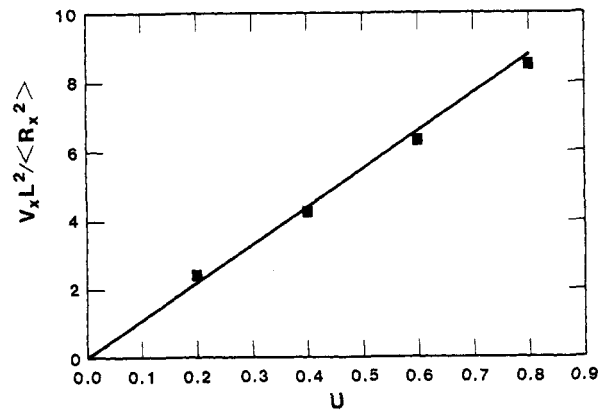

Figure 5. Plot using the functional dependence of the average center-of-mass velocity as predicted in eq 10. Points from simulation and line from theory with slope = $F_r/\zeta = 11$ used in simulation.

The dynamics of this system are now examined. Equation 10 and Figure 5 show that the quantity $V_x L^2 / \langle R_x^2 \rangle$ is proportional to U. The line drawn in Figure 5 has the theoretical slope of $F_r/\zeta = 11$, and agreement between theory and simulation is excellent. Therefore, the center-of-mass velocity, as predicted previously and shown experimentally,[10-12] is inversely proportional to molecular weight for low molecular weights and becomes independent of it at higher values. This loss of dependence on molecular weight implies an inability to separate species of different molecular weights by gel electrophoresis and is, therefore, extremely important.

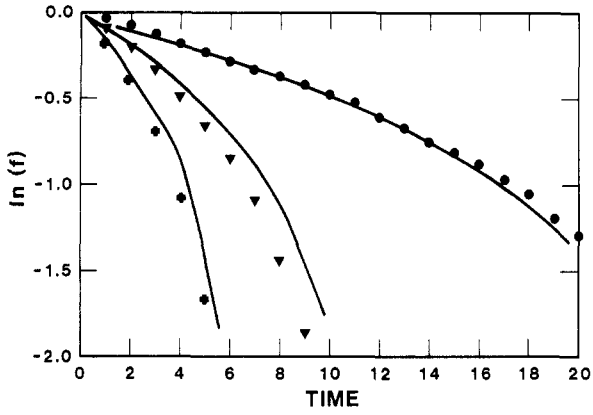

Figure 6. Normalized transverse component of the end-to-end vector correlation function from simulation with $N = 30$ (points for $U = 0.4$ (●), $U = 0.6$ (▼), and $U = 0.8$ (+)) and fraction of segments in the original tube from eq 25 (lines).

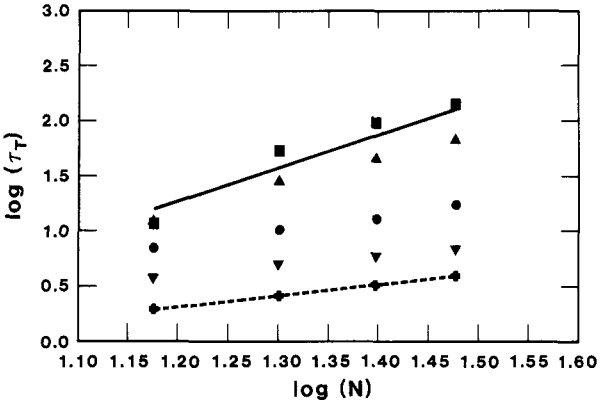

Figure 7. Simulation transverse relaxation time vs. number of beads for $U = 0$ (■), $U = 0.2$ (▲), $U = 0.4$ (●), $U = 0.6$ (▼), and $U = 0.8$ (+). Solid line has theoretical slope of 3 valid for $U = 0$, and dotted line has theoretical slope of 1 valid for large U.

As stated earlier, the transverse component of the end-to-end vector correlation function should be related to the fraction of segments still in the original tube, $F(t)$, given by eq 25. These two functions are compared in Figure 6 for $N = 30$ and $U = 0.4$, 0.6, and 0.8. τ_{rep} is defined as the relaxation time for $U = 0$ ($\tau_{rep} = 140$), and $\tau_e \sim (F_e\langle|R_x|\rangle)^{-1}$ is assumed to be proportional to U^{-2} by the results of Figure 4. Figure 6 shows that these two functions are qualitatively very similar and definitely nonexponential.

The simulation transverse relaxation time, defined as the time where the quantity $\langle R_y(0)R_y(t)\rangle/\langle R_y^2(0)\rangle = e^{-1}$, is plotted against U and N logarithmically in Figures 7 and 8. For $U = 0$, this relaxation time should be equal to $\tau_{rep} \sim N^3$. The solid line in Figure 7 has the theoretical slope of 3, and the simulation agrees fairly well with this prediction. The scatter here is not due to poor statistics, but to the error associated with rounding s/a to the nearest integer, which decreases as s/a increases (i.e., larger U). As U increases, the transverse relaxation time should approach $L/\langle\dot{s}\rangle \sim U^{-2}N$, where $\langle\dot{s}\rangle$ is defined in eq 24. Figures 7 (dotted line slope = 1) and 8 (solid line slope = −2) confirm this prediction and agree with the results of Figure 1.

The transverse center-of-mass diffusion coefficient is also plotted against U and N logarithmically in Figures 9 and 10. For $U = 0$, D_T should equal $D_{rep} \sim N^{-2}$. The solid line in Figure 9 has the theoretical slope of −2, and the simulation again agrees fairly well with this. The scatter is again associated with rounding s/a to the nearest integer. For large U, inspection of eq 18 shows that D_T should

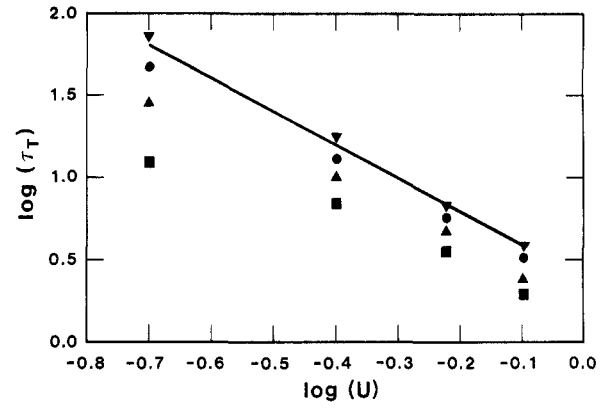

Figure 8. Simulation transverse relaxation time vs. field strength for $N = 15$ (■), $N = 20$ (▼), $N = 25$ (●), and $N = 30$ (▼). Line has theoretical slope of −2 valid for large U.

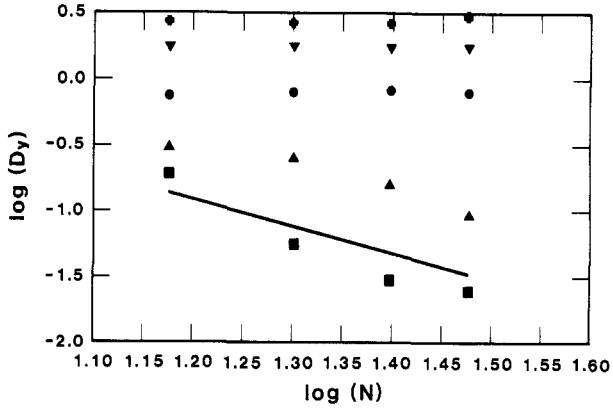

Figure 9. Simulation transverse component of center-of-mass diffusion coefficient vs. number of beads for $U = 0$ (■), $U = 0.2$ (▲), $U = 0.4$ (●), $U = 0.6$ (▼), and $U = 0.8$ (+). Line has theoretical slope of −2 valid for $U = 0$.

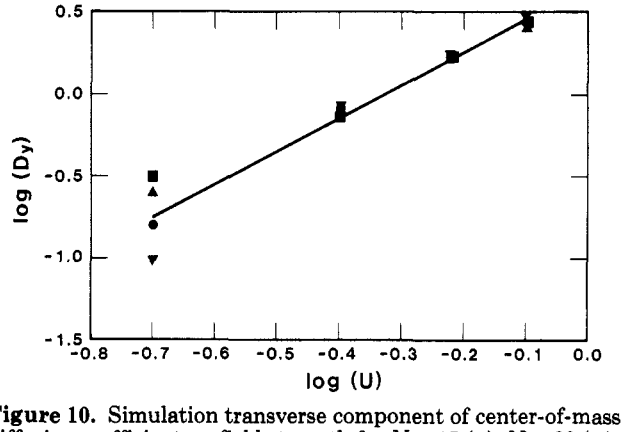

Figure 10. Simulation transverse component of center-of-mass diffusion coefficient vs. field strength for $N = 15$ (■), $N = 20$ (▲), $N = 25$ (●), and $N = 30$ (▼). Line has theoretical slope of 2 valid for large U.

become proportional to U^2 and independent of N if C is a constant. This is seen to be the case in Figures 9 and 10 (solid line slope = 2). To understand this, first notice that $\tau_P \gg \tau_T$, so $\tau_P\tau_T/(\tau_P + \tau_T) \approx \tau_T$. Now, using eq 18 and the high-field U, N dependencies of $\langle R_x^2\rangle \sim NU^2$, $\tau_T \sim \tau_e \sim N/U^2$, and $\langle R_y^2\rangle \sim N$, we see that C, as defined by

$$C = (\zeta/UF_r)^2(D_y - D_{rep}\langle R_y^2\rangle/\langle R_y^2\rangle_0) \approx \langle R_x\rangle^2\langle R_y^2\rangle\tau_T/L^4 \quad (26)$$

should be a constant for strong fields. In fact, C is very

nearly constant for all U values simulated. From simulation results, $C = 0.0345 \pm 0.0021$ averaged over all U,N runs. Therefore, the transverse diffusion coefficient for these parameter values is well approximated by

$$D_y = D_{rep}\langle R_y^2\rangle/\langle R_y^2\rangle_0 + C(UF_r/\zeta)^2 \quad (27)$$

where C is a material constant. Equation 27 states that the transverse diffusion coefficient in strong fields can be much larger than the zero-field purely reptational values.

The parallel component of the center-of-mass displacement is quickly dominated by the $V_x^2t^2$ term in eq 17, which makes it difficult to separate out the diffusive contribution in the simulation. However, eq 18 shows that $D_x = D_{rep}\langle R_x^2\rangle/\langle R_x^2\rangle_0$ when $U = 0$, and the quantity $\langle R_x^4\rangle - \langle R_x^2\rangle^2$ vanishes when U is large. Therefore, to a good approximation D_x equals $D_{rep}\langle R_x^2\rangle/\langle R_x^2\rangle_0$ for all U and is not nearly as affected by the external field as the transverse component. For large U, $\langle R_x^2\rangle/\langle R_x^2\rangle_0 \sim N$, so $D_x \sim N^{-1}$, in contrast to the zero-field result, $D_{rep} \sim N^{-2}$.

Conclusions

The present approach describing the dynamics of an entangled chain in an external field is extremely straightforward and can be directly used in computer simulations. Reptation is seen as a consequence of a balance of viscous drag and Brownian motion forces acting on a chain trapped in a tube. The addition of an external field results in a nonzero average center-of-mass velocity equivalent to that given by Lumpkin et al.[3,4] and Slater and Noolandi.[5,6] The center-of-mass diffusion coefficients were also derived in general form and simplified by using computer simulation results. The transverse diffusion coefficient is greatly affected by the external field, which would significantly broaden a pulse introduced into a gel electrophoresis column in a direction perpendicular to the external field. However, the parallel diffusion coefficient is less affected, so that separation of DNA molecular weights by gel electrophoresis is not hindered by excessive pulse broadening in a direction parallel to the external field.

The fraction of segments still in the original tube at time t was derived by using the analogous one-dimensional Smoluchowski equation to represent the diffusion of a segment in its tube in the presence of an external force acting tangential to the tube. This is seen to be quantitatively similar to the end-to-end vector correlation function examined in the computer simulations.

Acknowledgment. I thank J. Martin, M. Tirrell, G. Slater, and B. Zimm for helpful discussions and M. Olvera de la Cruz for excerpts of her doctoral thesis.

References and Notes

(1) de Gennes, P.-G. *Scaling Concepts in Polymer Physics*; Cornell University: Ithaca, NY, 1979.
(2) Tirrell, M. *Rubber Chem. Technol.* **1984**, *57*, 523.
(3) Lumpkin, O. J.; Zimm, B. H. *Biopolymers* **1982**, *21*, 2315.
(4) Lumpkin, O. J.; Dejardin, P.; Zimm, B. H. *Biopolymers* **1985**, *24*, 1573.
(5) Slater, G. W.; Noolandi, J. *Phys. Rev. Lett.* **1985**, *55*, 1579.
(6) Slater, G. W.; Noolandi, J. *Biopolymers* **1985**, *24*, 2181.
(7) Lerman, L. S.; Frisch, H. L. *Biopolymers* **1982**, *21*, 995.
(8) Olvera de la Cruz, M.; Deutsch, J. M.; Edwards, S. F. *Phys. Rev. A* **1986**, accepted for publication.
(9) Doi, M.; Edwards, S. F. *J. Chem. Soc., Faraday Trans. 2* **1978**, *74*, 1789.
(10) Southern, E. M. *Anal. Biochem.* **1979**, *100*, 319.
(11) Fangman, W. L. *Nucleic Acids Res.* **1978**, *5*, 653.
(12) McDonell, M. W.; Simon, M. W.; Studier, F. W. *J. Mol. Biol.* **1977**, *110*, 119.
(13) Verdier, P. H.; Stockmayer, W. H. *J. Chem. Phys.* **1962**, *36*, 227.
(14) Evans, K. E.; Edwards, S. F. *J. Chem. Soc., Faraday Trans. 2* **1981**, *77*, 1891.
(15) Uhlenbeck, G. E.; Ornstein, L. S. In *Selected Papers on Noise and Stochastic Processes*; Wax, N., Ed.; Dover: New York, 1954.
(16) Bird, R. B.; Hassager, O.; Armstrong, R. C.; Curtiss, C. F. *Dynamics of Polymeric Liquids*; Wiley: New York, 1977; Vol. 2.
(17) Chandrasekhar, S. In *Selected Papers on Noise and Stochastic Processes*; Wax, N., Ed.; Dover: New York, 1954.
(18) Graessley, W. W. *Adv. Polym. Sci.* **1982**, *47*, 67.

Computer Simulations of Simple Models of the Ring-Flip Process in Polycarbonate

Dennis Perchak*

Department of Macromolecular Science, Case Western Reserve University, Cleveland, Ohio 44106

Jeffrey Skolnick† and Robert Yaris

Institute of Macromolecular Chemistry, Washington University, St. Louis, Missouri 63130.
Received June 19, 1986

ABSTRACT: In order to investigate further the mechanism of the phenyl ring motion put forth by Schaefer et al. (Schaefer, J.; Stejskal, E. O.; Perchak, D.; Skolnick, J.; Yaris, R. *Macromolecules* **1985**, *18*, 368), Brownian dynamics computer simulations on two-dimensional lattices of interacting benzene rings have been performed. Two versions of this model were studied. One was a "rigid" lattice, which only allowed rotational motions of the rings, and the other was a "flexible" lattice, where vibrational motion of the rings was also allowed in the lattice plane. Consistent with the conjecture of Schaefer et al., for the simple models studied, flexibility in the lattice provided the mechanism that allowed rings to flip.

I. Introduction

Recently, much attention has been paid to molecular motions in glassy polycarbonate (PC) and polycarbonate-like materials.[1-7] Specifically, interest has focused on the fact that the dominant motion in PC is 180° "flips" of the phenyl rings about the C_1–C_4 axis. This has been regarded as being somewhat surprising since conformational energy calculations of an isolated PC chain[8] do not demonstrate a clear source for a two-state type of potential. In fact, these calculations indicate that the rings should be nearly free rotors at room temperature. Similar instances of 180° ring flips have also been observed in other

* Author to whom correspondence should be addressed.
† Alfred P. Sloan Foundation Fellow.

0024-9297/87/2220-0121$01.50/0